A laboratory experiment to test the limits of Bernoulli-Euler theory for flexural waves in bars

Brian E. Anderson

Citation: Proc. Mtgs. Acoust. **29**, 025004 (2016); doi: 10.1121/2.0000805
View online: https://doi.org/10.1121/2.0000805
View Table of Contents: http://asa.scitation.org/toc/pma/29/1
Published by the Acoustical Society of America

Proceedings of Meetings on Acoustics

Volume 29 http://acousticalsociety.org/

172nd Meeting of the Acoustical Society of America

Honolulu, Hawaii

28 November - 2 December 2016

Education in Acoustics: Paper 1aED2

A laboratory experiment to test the limits of Bernoulli-Euler theory for flexural waves in bars

Brian E. Anderson

Department of Physics & Astronomy, Brigham Young University, Provo, Utah, 84602; bea@byu.edu

At Brigham Young University, one of the acoustics courses taught in the Physics and Astronomy Department focuses on resonance topics. This course is a graduate level course that uses a differential equation approach to wave motion and resonances on strings, bars, membranes, and plates. This paper discusses the theory of flexural, or bending, waves in free-free rods and describes a laboratory experiment to test the rod thickness limits of the Bernoulli-Euler theory for rods. It is found that the fundamental frequency departs from Bernoulli-Euler theory as the thickness exceeds 6% of a flexural wavelength, however the mode shape above this limit remains unchanged (at least for the rods tested which included thicknesses up until the thickness equals 16% of a wavelength).

Published by the Acoustical Society of America

 https://doi.org/10.1121/2.0000805

1. INTRODUCTION

There are several type of modes that can exist at low frequencies in a bar (also referred to as a rod or a beam). These include longitudinal modes, torsional modes, and bending modes. A classic vibration topic in upper division physics or engineering undergraduate courses or introductory graduate level courses is the boundary value problem analysis of these modes (see chapter 3 in Ref. 1, Chapter 1 in Ref. 2, and chapter 5 in Ref. 3 for example coverage in textbooks aimed at this level). A bar is assumed to have cross sectional dimensions that are small compared to a wavelength, such that the vibrational dependence is strictly along the length of the bar.

A basic demonstration of longitudinal waves in a bar is the so called "singing rods" demonstration.[4-9] The demonstrator takes a long and thin bar (typically aluminum and of about 2 m length) and supports the bar in the middle with their thumb and index finger (or middle finger). The demonstrator then grips the bar with their thumb and index finger and slides their fingers along one end of bar to excite a longitudinal mode. Anderson showed that torsional and bending modes may also be excited and a nonlinear interaction can be observed depending on the length of the bar.[9]

Garrett described an electromagnetic excitation technique that allows independent excitation and sensing of longitudinal, torsional, and bending modes in free-free bars through the use of coils of wire that are bonded onto the ends of the bars.[10] The coils are each placed between the poles of two permanent magnets. This work also demonstrated how the added mass of the coils could be accounted for in each type of mode. Shortly thereafter, Rossing and Russell described a similar, inexpensive experiment intended for classroom demonstrations and laboratory exercises in which a small magnet is attached to a bar and is also driven electromagnetically by a small coil of wire placed just above where the magnet is attached to the bar.[11] The placement of the magnet (and coil) determines where the bar is pushed and pulled and thus different types of modes may be excited. A microphone was then suggested as the sensor to determine the resonance frequencies. Additional means of exciting resonances of the bar include eddy currents in electrically conducting bars,[12] electromagnetic-acoustic transducers,[13] and piezoelectric transducers.

The purpose of this paper is to describe a laboratory experiment to explore the limits of Bernoulli-Euler theory in determining the resonance frequency of a transversely vibrating bar. An analysis can be done to compare the resonance frequency of the fundamental mode of the bar as a function of thickness and/or length. Additional experiments may include the use of a Scanning Laser Doppler Vibrometer (SLDV) to image the vibrational shapes of bending modes and explore the agreement between theoretical and experimental mode shapes as a function of the thickness or length of the bar.

This paper will provide the theoretical equations for the resonance frequencies, nodal positions, and the relationship of the first four partials, relative to the fundamental frequency, for bars with many different combinations of boundary conditions. Then a discussion of laboratory exercises will be given and finally some concluding remarks.

2. THEORY

Bernoulli-Euler theory is typically used to teach bending wave modes. As the thickness of the bar becomes comparable to a wavelength, Timoshenko theory, which includes the effects of shear deformation and rotary inertia, should be used.[14] The development of the wave equation for bending waves in a bar is given in several textbooks, including Kinsler *et al.*,[1] Fahy and Gardonio,[2] and Garrett.[3] The wave equation is fourth order in space for the restoring force and second order in time for the inertial force

$$\frac{\partial^2 y}{\partial t^2} = -\kappa^2 c^2 \frac{\partial^4 y}{\partial x^4}, \tag{1}$$

where y is the amplitude along the bar, which is a function of position, x, and time, t. Additionally, κ is the radius of gyration ($\kappa = \frac{h}{\sqrt{12}}$ for a rectangular cross-section bar of thickness h or $\kappa = \frac{d}{4}$ for a circular cross-section bar of diameter d), and c is the bar longitudinal wave speed

$$c = \sqrt{\frac{E}{\rho}}, \tag{2}$$

where E is Young's modulus of elasticity and ρ is the mass density of the bar material.

There are three main types of boundaries for each end of the bar: free, simply supported (knife edge or hinged), or clamped, each with two boundary conditions. A free boundary implies that the end is unconstrained. A free end cannot cause that end to bend, meaning there is no resistance to angular acceleration (no moment), and thus at the boundary, x_B, $\frac{\partial^2}{\partial x^2} y(x_B, t) = 0$. A free end also cannot supply any vertical force, $\frac{\partial^3}{\partial x^3} y(x_B, t) = 0$. A simply supported boundary is supplied by two constraining knife edges that hold onto the top and bottom of the bar. These constraints do not allow this end to be displaced and thus $y(x_B, t) = 0$. Similar to the free end, the simply supported boundary also cannot supply any resistance to angular acceleration and thus $\frac{\partial^2}{\partial x^2} y(x_B, t) = 0$. Finally, a clamped boundary is supplied by some portion of the length of the bar being clamped, where this segment that is clamped is not included in the specification of the bar's vibrating length. Or a clamped boundary can be provided by gluing the end of the bar to a wall that is perpendicular to the bar's end, such that the cross section always remains perpendicular to the bar's axis. This means that the clamped boundary ensures no displacement of the end $y(x_B, t) = 0$ and the end must have a slope of zero at the boundary to keep the cross section at the end perpendicular to the bar's axis $\frac{\partial}{\partial x} y(x_B, t) = 0$.

If we assume time harmonicity, such that $y(x, t) = \Psi(x) e^{j\omega t}$ where $\Psi(x)$ represents the spatial dependence of the amplitude along the bar, $j = \sqrt{-1}$, and ω is the angular frequency, then the wave equation reduces to

$$\frac{\partial^4 \Psi}{\partial x^4} - \frac{\omega^2}{\kappa^2 c^2} \Psi = 0. \tag{3}$$

The trial solution for Eq. (3) must include functions whose fourth derivatives are proportional to those same functions, such as the orthogonal set of sine, cosine, hyperbolic sine, and hyperbolic cosine,

$$\Psi(x) = A \cosh gx + B \sinh gx + C \cos gx + D \sin gx, \tag{4}$$

where $g = \pm\sqrt{\frac{\omega}{\kappa c}}$ (the units of g suggest that it is a wavenumber quantity). It should be noted that the phase speed of waves in the bar, sometimes called the bending wave speed, is often defined such that

$$c_{ph} = \pm\sqrt{\kappa c \omega} = \pm\sqrt{\omega h \sqrt{\frac{E}{12\rho}}}. \tag{5}$$

Application of the appropriate two boundary conditions for each end of the bar (for example at $x_{B,1} = 0$ and at $x_{B,2} = L$, where L is the length of the bar) yields a transcendental equation. Solutions to the transcendental equation provide allowable values of the product $g_n L$ for the nth bending mode of the bar. The modal frequencies are then

$$f_n = \frac{1}{2\pi} \frac{\kappa c}{L^2} (g_n L)^2. \tag{6}$$

In the course of solving for the transcendental equation for a given bar, the constants A, B, C, and D are determined in relation to each other, leaving one constant that is determined by the initial conditions.

The free-free bar's transcendental equation is

$$(\sinh gL + \sin gL)(\sinh gL - \sin gl) = (\cosh gL - \cos gL)^2, \tag{7}$$

and the first four solutions are

$$g_{1-4} L = 4.73, 7.85, 11.00, \text{and } 14.14. \tag{8}$$

The first four modal frequencies of the free-free bar are

$$f_{1-4} = 3.56 \frac{\kappa c}{L^2} (1, 2.76, 5.40, \text{and } 8.93). \tag{9}$$

The spatial dependence for the free-free bar is

$$\Psi(x) = A[\cosh g_n x + \cos g_n x] - \frac{(\sinh g_n L + \sin\ _n L)}{(\cos\ _n L - \cos g_n L)} A[\sinh g_n x + \sin g_n x]. \quad (10)$$

For the first free-free bar mode, there are nodes at $0.224L$ and $0.776L$. For the second mode, there are nodes at $0.132L$, $0.5L$, and $0.868L$. For the third mode, there are nodes at $0.094L$, $0.356L$, $0.644L$, and $0.906L$. For the fourth mode, there are nodes at $0.073L$, $0.277L$, $0.5L$, $0.723L$, and $0.927L$.

The simply supported-simply supported bar's transcendental equation is

$$\sin gL = 0, \quad (11)$$

and the first four solutions are

$$g_{1-4}L = \pi, 2\pi, 3\pi, \text{and } 4\pi. \quad (12)$$

The first four modal frequencies of this bar are

$$f_{1-4} = \frac{\pi}{2}\frac{\kappa c}{L^2}(1, 4, 9, \text{and } 16). \quad (13)$$

The spatial dependence for the bar is

$$\Psi(x) = A \sin g_n x. \quad (14)$$

For the first mode, there are nodes at 0 and L. For the second mode, there are nodes at 0, $0.5L$, and L. For the third mode, there are nodes at 0, $0.333L$, $0.667L$, and L. For the fourth mode, there are nodes at 0, $0.25L$, $0.5L$, $0.75L$, and L.

The clamped-clamped bar's transcendental equation is identical to that of the free-free bar and the first four solutions are also identical. The first four modal frequencies of this bar are also identical to the free-free bar. The spatial dependence for the bar is

$$\Psi(x) = A[\cosh g_n x - \cos g_n x] + \frac{(\cosh\ _n L - \cos g_n L)}{(\sinh g_n L - \sin g_n L)} A[-\sinh g_n x + \sin g_n x]. \quad (15)$$

For the first mode, there are nodes at 0 and L. For the second mode, there are nodes at 0, $0.5L$, and L. For the third mode, there are nodes at 0, $0.358L$, $0.641L$, and L. For the fourth mode, there are nodes at 0, $0.279L$, $0.5L$, $0.721L$, and L.

The simply supported-free bar's transcendental equation is

$$\tan gL = \tanh gL, \quad (16)$$

and the first four solutions are $g_{1-4}L = 3.93, 7.07, 10.21, \text{and } 13.35$. The first four modal frequencies of this bar are

$$f_{1-4} = 2.46\frac{\kappa c}{L^2}(1, 3.24, 6.75, \text{and } 11.54). \quad (17)$$

The spatial dependence for the bar is

$$\Psi(x) = A \sinh g_n x - \frac{\cosh g_n L}{\cos g_n L} A \sin g_n x. \quad (18)$$

For the first mode, there are nodes at 0 and $0.736L$. For the second mode, there are nodes at 0, $0.446L$, and $0.853L$. For the third mode, there are nodes at 0, $0.308L$, $0.617L$, and $0.898L$. For the fourth mode, there are nodes at 0, $0.235L$, $0.471L$, $0.707L$, and $0.922L$.

The simply supported-clamped bar's transcendental equation is the same as that for the simply supported-free bar and the first four solutions are also identical. The first four modal frequencies of this bar are also identical to the simply supported-free bar. The spatial dependence for the bar is

$$\Psi(x) = A \sinh g_n x + \frac{\cosh g_n L}{\cos g_n L} A \sin g_n x. \quad (19)$$

For the first mode, there are nodes at 0 and L. For the second mode, there are nodes at 0, $0.442L$, and L. For the third mode, there are nodes at 0, $0.308L$, $0.614L$, and L. For the fourth mode, there are nodes at 0, $0.235L$, $0.471L$, $0.705L$, and L.

The clamped-free bar's transcendental equation is

$$(\sinh gL + \sin gL)(\sinh gL - \sin gl) = (\cosh gL + \cos gL)^2, \quad (20)$$

and the first four solutions are

$$g_{1-4}L = 1.88, 4.69, 7.85 \text{ and } 11.00. \quad (21)$$

The first four modal frequencies of this bar are

$$f_{1-4} = 0.56\frac{\kappa c}{L^2}(1, 6.22, 17.44, \text{and } 34.2). \quad (22)$$

The spatial dependence for the bar is

$$\Psi(x) = A[\cosh g_n x - \cos g_n x] + \frac{(\cosh {}_nL + \cos {}_nL)}{(\sinh {}_nL + \sin {}_nL)} A[-\sinh g_n x + \sin g_n x]. \quad (23)$$

For the first mode, there is one node at 0. For the second mode, there are nodes at 0 and $0.784L$. For the third mode, there are nodes at 0, $0.504L$, and $0.868L$. For the fourth mode, there are nodes at 0, $0.358L$, $0.644L$, and $0.906L$.

In all cases the fundamental resonance frequency increases linearly with increasing thickness (or diameter), decreases as $1/L^2$, and increases linearly with increasing c. For a given length, the clamped-free bar has the lowest fundamental frequency, followed by the simply supported-simply supported bar, then the simply supported-free and the simply supported-clamped bars, and then the free-free and clamped-clamped bars have the highest fundamental frequency. The bar with the highest amount of inharmonicity (deviation of upper partials with respect to integer multiples of the fundamental frequency) is the clamped-free bar, followed by the free-free and clamped-clamped bars, and then the simply supported-free and simply supported-clamped bars have the least degree of inharmonicity. The simply supported-simply supported bar has partials that are integer multiples of the fundamental but they are not integer multiples, but rather the square of integer multiples, thus this bar is still considered to have inharmonic partials with, in fact, the highest degree of departure from integer multiples. It is worth noting that longitudinal and torsional vibration modes of a bar are harmonically related to their respective fundamental frequencies.

It is interesting to ask students what they would expect to happen to the pitch of a transversely vibrating free-free bar if you have bars of the same length but different thicknesses (and the same widths). Almost always the student guesses that the thicker bar will have the lower fundamental frequency. Students must be relying on their intuition that suggests that an increased thickness means an overall increase in the mass of the bar, and an increase in mass should lower the resonance frequency, as it does for the single degree of freedom mass-spring system. The volume of the bar increases linearly with thickness and thus the mass of the bar would as well. However, in order to obtain the proportional relationship between the fundamental resonance frequency and thickness, the bending wave resonances of these bars increase linearly with increasing thickness, suggesting that the stiffness in the bar must be increasing as the cube of the thickness, while the mass is only increasing proportionally to the thickness, since $f \propto \sqrt{\frac{\text{stiffness}}{\text{mass}}} = \sqrt{\frac{h^3}{h}} = h$. In fact Fahy and Gardonio show that the bending stiffness is proportional to h^3 and the mass per unit area is proportional to h.[2] Students seem to always guess correctly that the pitch of the fundamental decreases with increasing length, since the pitch of most resonators decreases with increasing length.

3. LABORATORY ASSIGNMENT

For this suggested laboratory assignment, students should be provided with various bars of the same length and width but different thicknesses. For the laboratory exercise that was developed at Brigham Young University bars were purchased that were 30.48 cm in length (12 inches) and 7.62 cm in width (3 inches). Ten aluminum bars of various thicknesses were purchased, as shown in Fig. 1. Assuming $E = 71$ GPa and $\rho = 2700$ kg/m^3, the fundamental resonance frequencies may be calculated for free-free boundary conditions using Eq. (9). Table 1 displays the thicknesses, calculated wave speeds, and calculated fundamental frequencies.

Figure 1. Photograph of the 10 aluminum bars of different thicknesses.

Table 1. Thicknesses, wave speeds, and fundamental frequencies of the bars tested.

Bar Thickness (cm)	Bar Thickness (inches)	Bending Wave Speed (m/s)	Calculated Fundamental Frequency (Hz)	Measured Fundamental Frequency (Hz)	% Error in the Fundamental Frequency
0.32	1/8	73	180	183	1.3
0.63	1/4	146	360	355	-1.5
0.95	3/8	219	540	528	-2.4
1.25	1/2	292	721	728	1.0
1.59	5/8	365	901	913	1.3
1.90	3/4	438	1081	1100	1.8
2.54	1.00	584	1441	1428	-0.9
3.81	1.50	875	2161	2091	-3.3
5.08	2.00	1167	2882	2666	-7.5
7.62	3.00	1750	4323	3731	-13.7

The measured frequencies can be determined by striking the bar near an antinode position while supporting it at the node positions for the fundamental mode or by driving the bar with a shaker using a sweep or random noise signal. Fishing line was used to support the bars in this experiment as shown in Fig. 1 and driven with a shaker as shown in Fig. 2. We chose to drive the shaker at the middle of the bar, which is an antinode for the fundamental mode. An SLDV was aimed at an antinode position at the end of the bar (the laser spot is visible on the left side of the bar in Fig. 2. The bars were each driven with a sine sweep signal and the measured fundamental frequencies are tabulated in Table 1. The percent error between the calculated modal frequencies and the measured modal frequencies is also given in Table 1. Note that the error is sometimes above or below the expected value up until a thickness of about 3.81 cm and then the bars yield consistently lower measured fundamental frequencies than the calculated frequencies. Figure 4 displays the calculated and measured fundamental frequencies as a function of thickness.

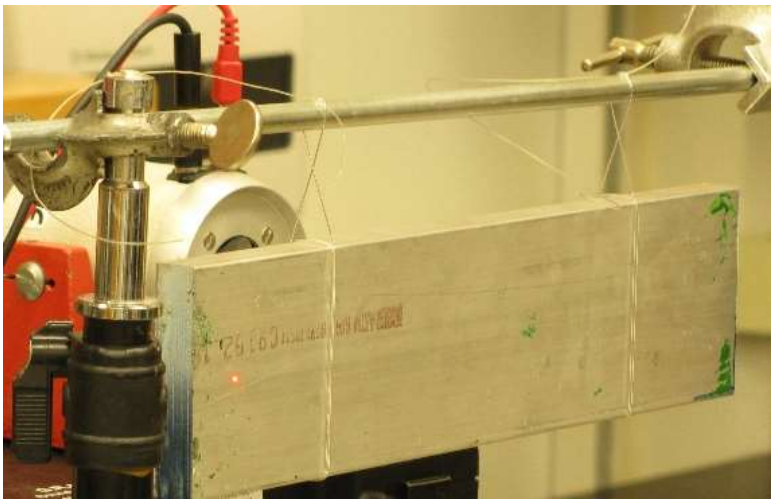

Figure 2. Photograph of a bar under test suspended by fishing line at the nodal positions.

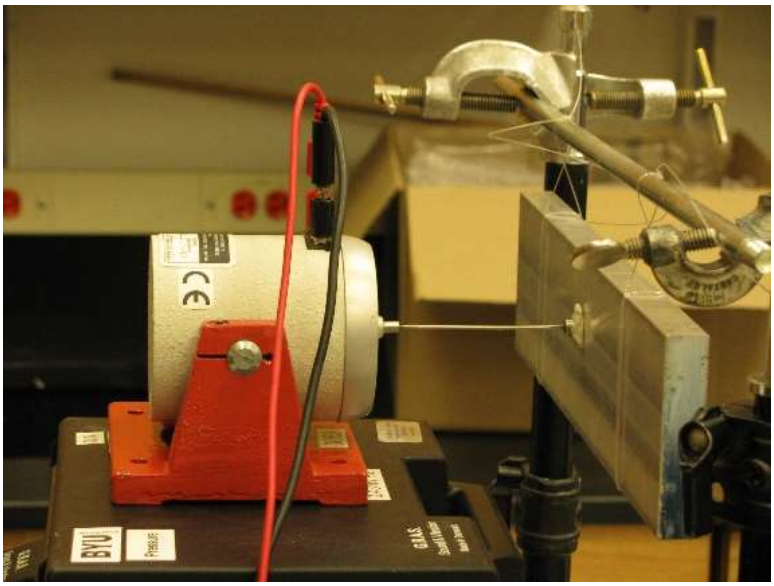

Figure 3. Photograph of the bar under test being driven by a shaker.

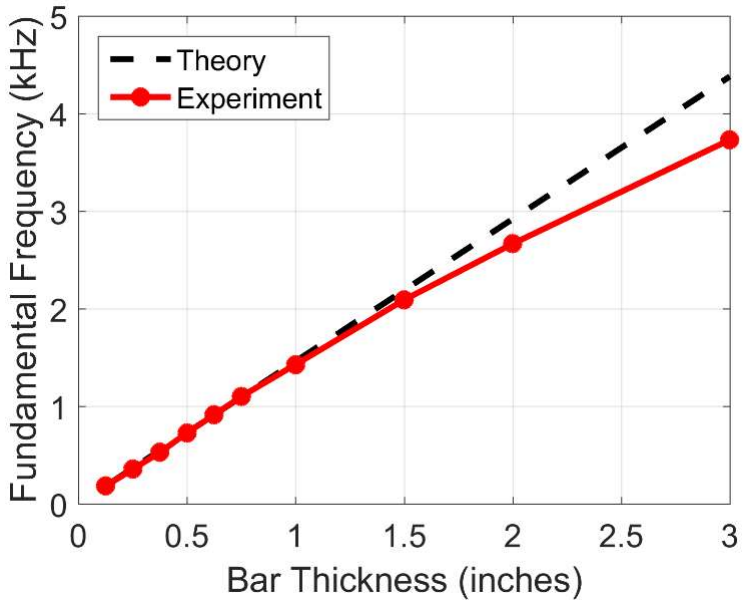

Figure 4. Photograph of the bar under test being driven by a shaker.

The SLDV was then used to scan along the center line of the bar from free end to free end while the shaker is driven by a sine wave at the measured fundamental frequency. The SLDV triggers off of the sine wave excitation signal so that the measurements at each position along the length of the bar can be synchronized to simulate measuring at every position along the bar length simultaneously. The mode shapes for the fundamental frequency are then plotted in Fig. 5, all with the same phase. The theoretical mode shape from Eq. (10) is also plotted in Fig. 5. As is clear from an observation of Fig. 5, all of the mode shapes match the theoretical mode shapes extremely well aside from background noise since all of the mode shapes are displayed on top of each other. It should be noted that the mode shapes have all been normalized to compare the shapes of the modes.

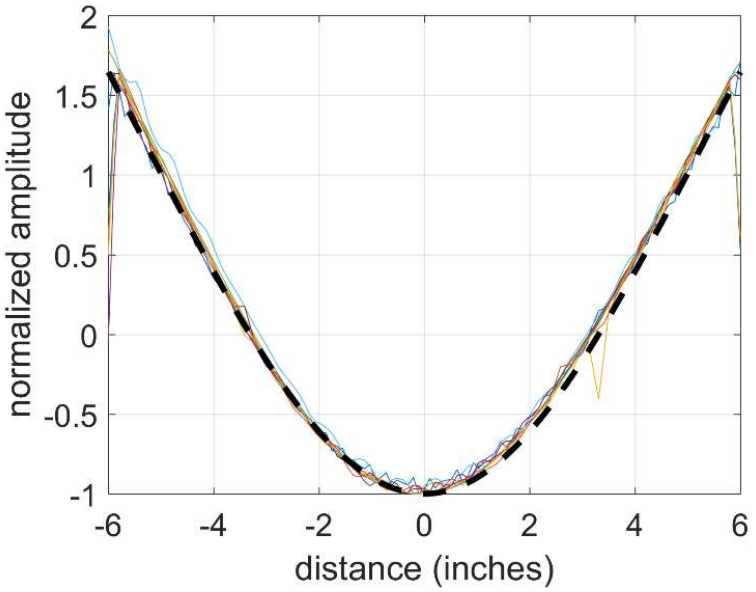

Figure 5. Measured fundamental frequency mode shapes for each of the ten bars measured (various thin solid lines of different colors) along with the theoretical mode shape (black dashed line), displayed as instantaneous amplitudes versus distance along the bars' lengths.

The laboratory assignment can ask the students to determine at what point the Bernoulli-Euler theory breaks down for the measured fundamental frequencies. The apparent departure from the theory increases with thickness beginning at a thickness of 3.81 cm (1.5 inches), meaning that above a thickness of 2.54 cm (1 inch) the theory breaks down. Students can also be asked to calculate the highest expected non-dimensional product of the bending wave wavenumber, $k = \frac{\omega}{c_{ph}}$, and the bar thickness at which the theory still holds. In this case, Table 1 suggests that this product equals $kh = \frac{2\pi(1441\text{ Hz})}{584\text{ m/s}}(0.0254\text{ m}) = 0.39$. A common rule of thumb is that Bernoulli-Euler theory breaks down above a value of $kh = 1$, but this exercise suggests that it breaks down at 0.39. This laboratory exercise also helps the students see that even though the measured fundamental frequencies are over predicted by Bernoulli-Euler theory, the mode shapes are still correct, at least for the bars measured here.

Additional assigned work could ask the students to compare the measured modal frequencies for modes above the fundamental to those predicted by theory. In this case the students should change the position of the fishing line supports and the drive point location since the middle of the bar is a node for all of the even numbered modes and the two outer most nodal positions (ideal for stable support the bar) move towards the free ends with increasing mode number.

4. CONCLUSION

This paper has reviewed the Bernoulli-Euler theory for bars with various combinations of boundary conditions, providing the transcendental equations, eigenvalues of said equations, the first four modal frequencies, the mode shapes, and the nodal positions. Since the free-free end conditions are the easiest to realize experimentally, various bars are measured in a free-free state. Results were presented for ten free-free bars of different thicknesses, including the measured fundamental frequencies and measured fundamental mode shapes. It was found that the Bernoulli-Euler theory breaks down at a value of $kh = 0.39$. It was also found that the measured mode shapes agree very well with the theory, even though the Bernoulli-Euler theory does not predict the frequencies exactly.

REFERENCES

[1] L. E. Kinsler, A. R. Frey, A. B. Coppens, and J. V. Sanders, Fundamentals of Acoustics, 4th Edition (John Wiley and Sons, Inc., New York, 2000), Ch. 3, p. 68-87.
[2] F. Fahy and P. Gardonio, Sound and Structural Vibration, 2nd Edition (Academic Press, Oxford, 2006), Ch. 1, p. 11-26.
[3] S. L. Garrett, Understanding Acoustics (Springer and ASA Press, New York, 2017), Ch. 5, p. 279-305.
[4] H. F. Meiners, Physics Demonstration Experiments (Ronald, New York, 1970), Vol. I, p. 496.
[5] N. Naba, "Observation of longitudinal vibration of metal rods," Am. J. Phys. 40(9), 1339–1340 (1972).
[6] R. C. Nicklin, "Measuring the velocity of sound in a metal rod," Am. J. Phys. 41(5), 734–735 (1973).
[7] R. B. Minnix, D. R. Carpenter, and W. W. McNairy, "How to make singing rods scream," 66th Annual Meeting of the Southeastern Section of the American Physical Society (November 7–9, 1999).
[8] R. Machorro and E. C. Samano, "How does it sound? Young interferometry using sound waves," The Phys. Teacher 46, 410–412 (2008).
[9] B. E. Anderson and W. D. Peterson, "The song of the singing rod," J. Acoust. Soc. Am. **131**(3), 2435-2443 (2011).
[10] S. L. Garrett, "Resonant acoustic determination of elastic moduli," J. Acoust. Soc. Am. **88**(1), 210-221 (1990).
[11] T. D. Rossing and D. A. Russell, "Laboratory observation of elastic waves in solids," Am. J. Phys. **58**(12), 1153- (1990).
[12] A. Morales, L. Gutiérrez, and J. Flores, "Improved eddy current driver-detector for elastic vibrations," Am. J. Phys. **69**(4), 517-522 (2001).
[13] J. A. Franco-Villafañe, E. Flores-Olmedo, G. Báez, O. Gandarilla-Carrillo, and R. A. Méndez-Sánchez, "Acoustic resonance spectroscopy for the advanced undergraduate laboratory," Eur. J. Phys. **33**(6), 1761 (2012).
[14] S. P. Timoshenko, "On the correction for shear of the differential equation for transverse vibrations of prismatic bars," Phil. Mag., Ser 6, **41**, 744-746 (1921).